

A new approach for nonlinear finite element analysis of reinforced concrete structures with corroded reinforcements

Mohsen A. Shayanfar*

*Civil Engineering Department, Iran University of Science and Technology,
Narmak 16846, Tehran, Iran*

Amir Safiey

*Moshanir Consultants Engineering Inc., Park Prince Buildings, Vanak, Tehran, Iran
(Received February 7, 2007, Accepted March 6, 2008)*

Abstract. A new approach for nonlinear finite element analysis of corroded reinforcements in reinforced concrete (RC) structures is elaborated in the article. An algorithmic procedure for producing the tension-stiffening curve of RC elements taking into consideration most of effective parameters, e.g.: the rate of steel bar corrosion, bond-slip behavior, concrete cover and amount of reinforcement, is illustrated. This has been established on both experimental and analytical bases. This algorithm is implemented into a nonlinear finite element analysis program. The abilities of the resulted program have been studied by modeling some experimental specimens showing a reasonable agreement between the analytical and experimental findings.

Keywords: nonlinear finite element method; reinforced concrete; tension-stiffening; bond-slip; corrosion.

1. Introduction

The integrity of many RC structures and infrastructures are compromised due to some dangerous effects of the aggression of the corrosive agents. To evaluate the effects of these types of the damages on the total behavior of reinforced concrete structures, the nonlinear finite element models for reinforced concrete need an improvement to take the effects of corrosion of the steel rebars into account. The importance of analytical models would be more highlighted by taking a glance on the expensive costs of experimental explorations. A survey on the literature reveals that there is a knowledge gap in this area of researches; relatively few studies addressed explicitly analytical modeling of corroded reinforcements in RC members. Hereunder, some of the published analytical models are reviewed:

- (i) *Coronelli and Gambarova (2004)*: Nonlinear finite element method has been used by these researchers. The concrete has been modeled by four node element and steel by bar element. In their modeling a bond-link element exhibiting a relative slip between two materials couples the concrete elements to corresponding bar element has been utilized for modeling of bond-slip behavior. The model takes into account the effects of corrosion on behavior of

* Associate Professor, Corresponding Author, E-mail: mohsenalishayanfar@gmail.com

steel and concrete by reducing the cross-sectional area of the bar element representing steel and size of mesh representing the concrete, and by modifying the constitutive laws of the material and of their interface. They verified their models with analysis of some simply supported RC beams.

- (ii) *Dekoster, et al. (2003)*: Dekoster, *et al.* studied flexural behavior of beams subjected to localized and uniform corrosion. In this research both elasto-plastic and damage approach have been utilized for concrete material and elasto-plastic model by isotropic hardening work had been used for steel material. They have used special elements to represent the bond between concrete and steel; they have called this type of element “rust element”. In the finite element computations, corrosion products have been considered as third component between concrete and steel; the rust has been assumed as elastic material that from properties point of view is similar to water. But the properties of these elements are varied along the rebar and surrounding concrete in order to model the non-localized corrosion and pitting. These researchers have found out that the load-deflection of flexural behavior dominant RC beams, are sensitive to size of “rust elements”.
- (iii) *Lundgren (2001)*: In the earlier work of Lundgren (1999), “a general model of the bond mechanism was developed. In this bond model, the splitting stresses of bond action are included, and the bond stress depends not only on the slip, but also on the radial deformation between the reinforcement bar and the concrete. Thereby, the loss of bond at splitting failure or if the reinforcement is yielding can be simulated.” Lundgren (2001) generalized the bond model for considering corrosion effects. For this purpose, a special layer for modeling of corrosion was introduced between concrete and rebar. Lundgren’s model is based on plasticity theory; a non-associated flow rule was assumed. Then, Lundgren completed the study by verifying the resulted model by modeling and analyzing the field corrosion-cracking tests and pull-out tests on corroded specimens and comparing the results; the comparison sounds reasonable but it seems that the analyses are restricted to study behavior of RC in small scale and they are not appropriate for studying the whole structure behavior.
- (iv) *Lee, et al. (2000)*: These researchers used nonlinear finite element analyses to predict the behavior of corroded reinforced concrete beams; the models were constituted from three types of elements representing: concrete, steel and bond. The bond was modeled by 4-node isoparametric plane element with an appropriate constitutive law.

All of the above mentioned models have their own advantages and disadvantages. Dekoster, *et al.* (2003), Coronelli and Gambarova (2004) and Lee, *et al.* (2000) researches sound to be more valuable from engineering point of view but Lundgren’s model (2001) seems to be more complicated and suitable at elemental level. The common point of these models is application of especial elements between concrete and reinforcement to represent the bond-slip behavior and associated damages as results of the effects of corrosion of reinforcements.

Corrosion of steel reinforcements in the RC structures diminishes the total load bearing capacity of RC structures, not only by means of rebar cross-sectional area reduction, but also by bond deterioration as reported by some of the researchers, e.g. Amleh and Mirza (1999). Tension-stiffening phenomenon in reinforced concrete is developed as a result of steel and concrete bond that occurs between the tensile cracks. Therefore, degrading effects of corrosion to the bond between steel and concrete could be taken into consideration by the tension stiffening models. Utilizing a proper tension stiffening model for these purposes might be a more practical method to

solve the problem which is not engaged in it by now in the state-of-the-art. Accordingly, a new bond-slip-tension-stiffening model considering the effects of corrosion of reinforcement was developed; it is described with numerical implementation details in the subsequent section. It is implemented into nonlinear finite element as a part of a hypoelastic model of reinforced concrete. The details of the analytical model are available in Shayanfar (1995). Finally, the performance of the program in handling nonlinear analysis of corroded reinforced concrete members is validated.

2. Proposed tension-stiffening model

In this section, a new bond-slip-tension-stiffening model is introduced. The model is established on both experimental and analytical bases; the analytical bases are used to attain some relationships between “crack spacing” and concrete stress and rebar strain contributions in tension. Experimental relationships are used to take into account the effects of some parameters such as “rate of corrosion” and “final crack point” in the proposed model. In the followings, the analytical and experimental backgrounds of the proposed tension stiffening model are reviewed. Afterwards, the computational aspects of the proposed model are also discussed.

2.1. Analytical background

In Fig. 1(a), a piece of RC specimen between two faces of adjacent cracks is shown; the parameter a is defined as half of spacing between two adjacent cracks. Concrete stress and steel strain contributions and bond stress distribution on reinforcement within two faces of adjacent cracks are depicted in Fig. 1. The basic need of the proposed tension stiffening model is some proper relationships between parameter a and concrete stress contribution and steel strain contribution. It is observed in the experimental studies (e.g. Ghalehovi 2004) that the tension stiffening curve of a concrete specimen can be divided into two distinct parts according to the associated bond-slip behavior, namely: “multiple cracking state” and “final cracking state” as shown

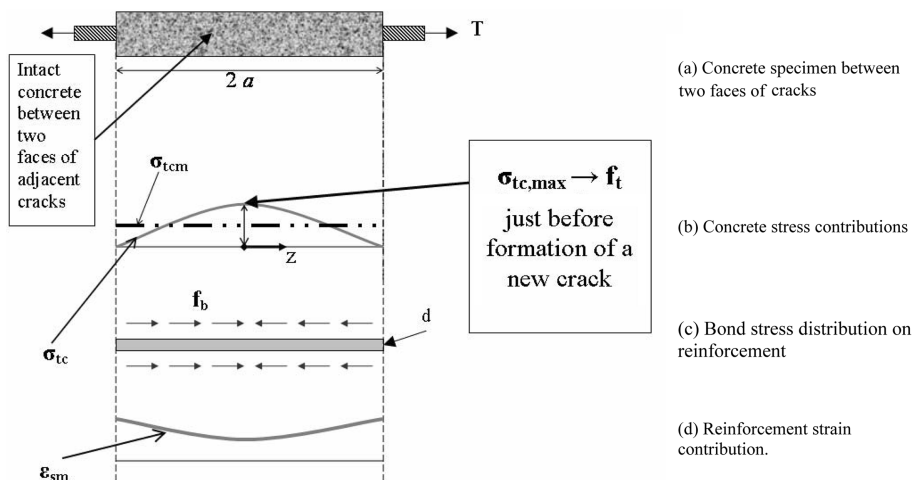


Fig. 1 Schematic representation of intact concrete between two faces of adjacent cracks

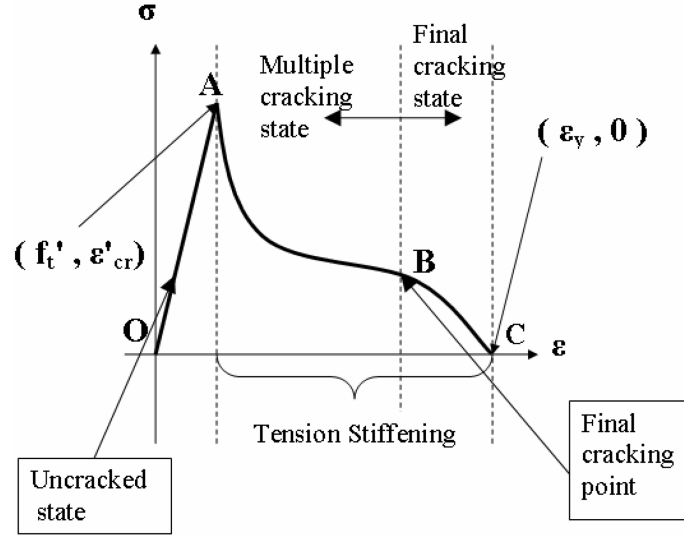


Fig. 2 Schematic representation of tension stiffening curve

schematically on Fig. 2; thereby, the aforementioned relationships should be obtained separately for “multiple cracking state” and “final cracking point”. These relationships are extracted as follows:

2.1.1. Multiple cracking state

In multiple cracking state, the assumption of linear bond-slip behavior complies with experimental observations (Ghalehnavi 2004). Uniform stress distribution over the specimen cross-section is assumed. Gupta and Maestrini (1990) studied concrete tension stiffening analytically. These researchers represented the results of compatibility and equilibrium of the steel bar and surrounding concrete differential equation closed form solutions by assumption of linear or constant bond-slip behavior. Concrete stress and force contribution with linear bond-slip behavior assumption according to Gupta and Maestrini (1990) are:

$$F_c = \frac{E_b \Psi C_1}{k} (\cos(ka) - \cosh(kz)); \quad C_1 = \frac{T}{A_s E_s k \cosh(ka)} \quad (1)$$

$$\sigma_{tc} = \frac{F_c}{A_c} = T \cdot \frac{\cosh(ka) - \cosh(kz)}{A_c (1 + n\rho) \cdot \cosh(ka)} \quad (2)$$

Some of the variables in the above equations are explained in Fig. 1; the constant parameter k is equal to $\sqrt{E_b \Psi (1 + n\rho) / A_s E_s}$; z is an axis perpendicular to crack direction and varies in $[-a, a]$ interval. Let assume $z=0$, the concrete stress contribution reaches to its maximum value at origin of z axis as:

$$\sigma_{tc, \max} = T \cdot \frac{\cosh(ka) - 1}{A_c (1 + n\rho) \cdot \cosh(ka)} \quad (3)$$

Just before formation of a new crack, the value of $\sigma_{tc, \max}$ reaches to concrete tensile strength, f_t , and Eqs. (2) and (3) can be rewritten in these forms:

$$T = f_t \cdot \frac{A_c(1+n\rho)\cosh(ka)}{\cosh(ka)-1} \tag{4}$$

$$\sigma_{ic} = f_t \cdot \frac{\cosh(ka)-\cosh(kz)}{\cosh(ka)-1} \tag{5}$$

In Eq. (4), T is requisite tensile force to develop a new crack in concrete. Since in the ordinary reinforced concrete finite element formulations, smeared concrete stresses and strains are used; it is necessary to find the value of average stress or strain contributions. Ghalehnovi (2004) proposed this trend for obtaining the mean values. The strain energy of the intact concrete piece between two faces of adjacent cracks can be computed as:

$$U_1 = 2 \int_0^a \frac{\sigma_{ic}^2}{2E_0} \cdot A_c \cdot dz \tag{6}$$

In the above equation, σ_{ic} is concrete stress contribution; that is a function of z according to Eq. (5). By assuming an imaginary uniform concrete stress distribution across the spacing between the two faces of the adjacent cracks-see Fig. 1(b) - the strain energy is:

$$U_2 = \frac{\sigma_{icm}^2}{2E_0} \cdot A_c \cdot (2a) \tag{7}$$

According to the principal of the conservation of energy and by neglecting energy losses, the results obtained by Eqs. (6) and (7) are identical and the average value of concrete stress contribution could be resulted as:

$$\sigma_{icm} = \frac{f_t}{\cosh(ka)-1} \sqrt{1+0.5\cosh(2ka)-0.75 \frac{\sinh(2ka)}{(ka)}} \tag{8}$$

Now, by considering the equilibrium for the average concrete and steel forces:

$$T = F_{sm} + F_{cm} = A_s E_s \varepsilon_{sm} + A_c \sigma_{icm} \tag{9}$$

The average steel strain contribution is resulted by:

$$\varepsilon_{sm} = \frac{1}{A_s E_s} (T - A_c \sigma_{icm}) \tag{10}$$

Where T could be computed by Eq. (4).

The Eqs. (8) and (10) play a key role in the proposed model. These relations are valid whenever the bond-slip behavior is linear or in “multiple cracking state”, just before formation of each new crack.

2.1.2. Final cracking point

The final cracking state is the next state on the tensile stress-strain curve of a RC member as shown in Fig. 2. According to the experimental observations (Ghalehnovi 2004) in this state, constant bond stress distribution is assumed across the reinforcement between two faces of adjacent cracks. In this state, the steel reinforcement has been started yielding from crack faces; therefore, the total tensile force, T , is equal to $A_s \cdot f_y$. Bond stress distribution, reinforcement force contribution, concrete force contribution and reinforcement strain contribution at this state are shown in Fig. 3. The

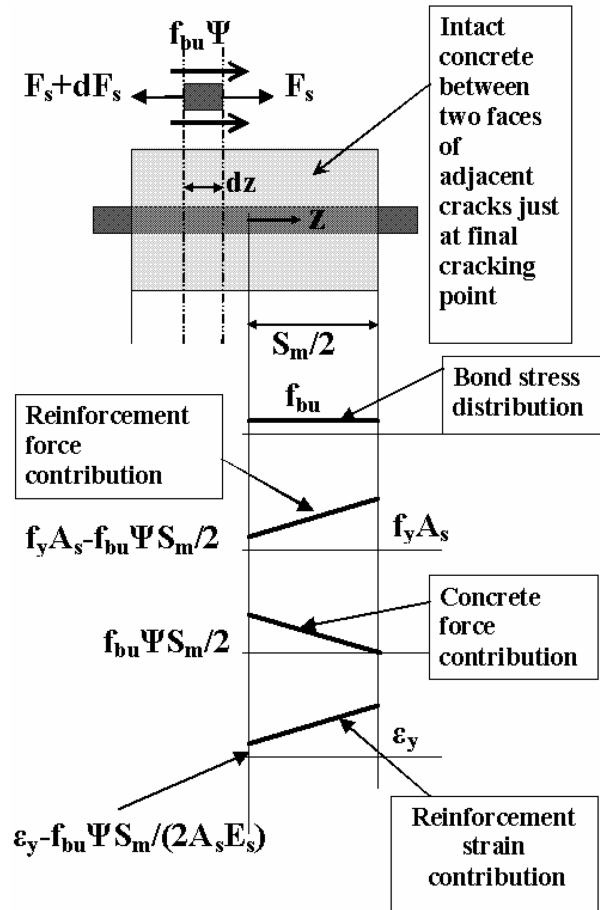


Fig. 3 A piece of the intact concrete at the “final cracking point”

common point between “multiple cracking state” and “final cracking state” is named “final cracking point” (see Fig. 2). From this point further, intact concrete between cracks becomes unable to reach its tensile strength. The equilibrium between the reinforcement force contribution and ultimate bond stress on the perimeter of the reinforcement for a small piece of reinforcement – see Fig. 3-provide the following differential equation:

$$\frac{dF_s}{dz} = \Psi \cdot f_{bu} \quad (11)$$

The above equation had been solved to achieve force contribution of steel reinforcement. Force contribution of concrete and steel are in balance with the total tensile force or $T = F_s + F_c$. Assumption of uniform distribution of concrete stress over the cross-section results in $\sigma_{ic} = F_c / A_c$. Finally, by utilizing these equations, the concrete stress distribution over the spacing between two faces of adjacent cracks could be formulated as:

$$\sigma_{ic} = \frac{f_{bu} \cdot \Psi(a-z)}{A_c} \quad (12)$$

Utilizing energy conservation principle and Eqs. (6), (7), the average concrete stress contribution at “final cracking point” is obtained:

$$\sigma_{icm} = \frac{f_{bu} \cdot \Psi \cdot S_m}{A_c \cdot 2\sqrt{3}} \quad (13)$$

It is noted in extracting the above equation, this fact has been used that at final cracking point: $a = S_m/2$. Using Eq. (10), the average reinforcement strain at “final cracking point” is resulted as:

$$\varepsilon_{sm} = \varepsilon_y - \frac{f_{bu} \cdot \Psi \cdot S_m}{A_s \cdot E_s \cdot 2\sqrt{3}} \quad (14)$$

Eqs. (13) and (14) show that S_m is the most crucial parameters in the process of switching from multiple cracking state to final cracking state. A comprehensive experimental program has been carried out to study this parameter and some of the other important parameters. Some of the results of this experimental investigation are presented in the following subsection.



Fig. 4 Experimental test setup

2.2. Experimental background

58 direct tension tests on corroded and noncorroded RC specimens have been conducted recently. The test setup is shown in Fig. 4; the results of the experimental investigation reported elsewhere (Ghalehnovi 2004). Some of the empirically obtained formulas are summarized as follows:

2.2.1. Average final crack spacing, S_m

At final cracking point, the intact concretes between the cracks become unable to reach the tensile strength, as remarked earlier; therefore, the spacing between the two faces of adjacent cracks remain unchanged until the failure of the specimen. For achieving a decisive factor to identify transition from “multiple cracking state” to “final cracking state”, the following experimental criterion was proposed:

$$S_m = 2.35c \cdot \begin{cases} 1 & C_w = 0 \\ 1.533 - 0.3\frac{c}{d_0} + 4.2\left(\frac{C_w \cdot d_0}{9c}\right)^2 & C_w > 0 \end{cases} \quad (15)$$

In Eq. (15), the “average final crack spacing”, S_m , means: the average of distances between adjacent cracks at “final cracking point” in a specific specimen, see Fig. 5. The above formula is extracted by least square curve fitting to the experimental results (see Fig. 6 as an example).

2.2.2. Steel reinforcement yield strain, ε_y

According to the experimental exploration, corrosion of steel reinforcement affects yield strain of rebar as below:

$$\varepsilon_y = \frac{f_y}{E_s} \cdot \begin{cases} 1 & C_w = 0 \\ 0.907 - 0.757\frac{C_w d_0}{9c} + 0.0087\frac{c}{d_0} & C_w > 0 \end{cases} \quad (16)$$

The above equation reveals that the sensitivity of steel reinforcement yielding strain to the certain degree of corrosion also depends on its diameter and concrete cover.

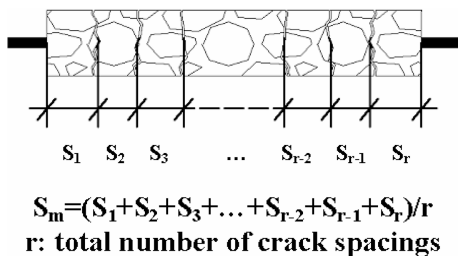


Fig. 5 Visualization of the concept of the average final crack spacing parameter

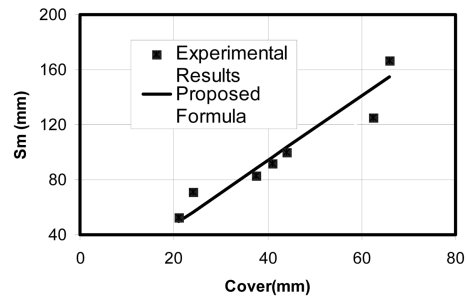


Fig. 6 A comparison between experimental observations for non-corroded RC specimens and the proposed formula

2.2.3. Reinforcement cross-sectional area, A_s

To consider the cross-sectional area reduction of the steel reinforcements due to corrosion, the following experimental equation has been utilized:

$$A_s = A_{s,0} \cdot \begin{cases} 1 & C_w = 0 \\ 1.2 - 0.35 \frac{C_w d_0}{9c} - 0.08 \frac{c}{d_0} & C_2 > 0 \end{cases} \quad (17)$$

The above formula takes into account the effects of non-uniform corrosion and pitting on the cross-sectional area.

2.2.4. Ultimate bond strength, f_{bu}

The ultimate bond strength between concrete and steel reinforcement was estimated by the following experimental relationship:

$$f_{bu} = \frac{0.4c}{d_0} \sqrt{f_c} \quad (18)$$

2.3. Tension stiffening model implementation

As it was noted earlier, the tension-stiffening curve consists of two distinct states, namely “multiple cracking state” and “final cracking state”; therefore, the uniaxial tensile stress-strain curve of a RC element could be divided into three states; see Fig. 2: (a) “uncracked state” (path OA) (b) “multiple cracking state” (path AB) and (c) “final cracking state” (path BC). The numerical strategy of the proposed model is to discretize the tensile stress-strain curve by a set of discrete points called “principal points”. Those are connected by straight line to form a polygon similar to Fig. 7. The number of “principal points”, N , is a constant value for a specific RC element during each analysis. This value probably differs from a RC element to another, depending on its characteristics; the minimum value of N is 4; because at least for describing the reinforced concrete tensile stress-strain

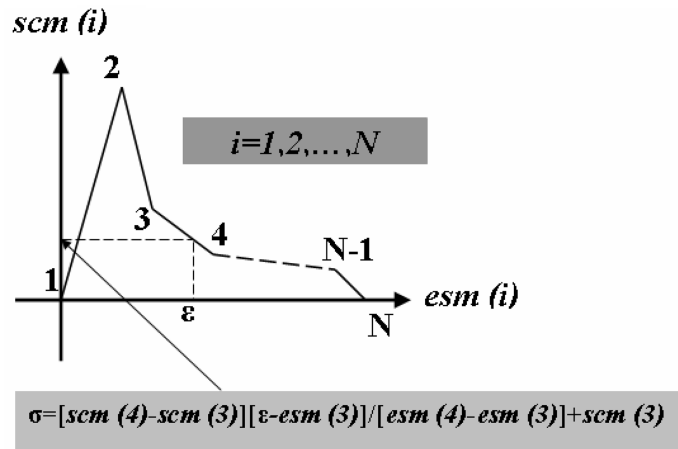


Fig. 7 Idealization of RC tensile behavior and a sample for linear interpolation between principal points

curve, three lines are necessary. The computed stress and strain values corresponding to “principal points” are stored in two separate vectors, namely: $\{esm\}$ and $\{scm\}$; the dimensions of these two vectors are equal to the number of “principal points”, N ; the detailed calculations associated to elements of these two vectors are represented in the following lines; the value of tensile stress corresponding to the specific tensile strain could be calculated by a linear interpolation. This concept and a sample for interpolation between the “principal points” are represented in Fig. 7.

For $i=1$, the values $esm(i=1)$ and $scm(i=1)$ are equal to zero. When $i=2$, the values $esm(i=2)$ and $scm(i=2)$ are equal to ε'_{cr} and f'_t ; when i exceeds 2 the “multiple cracking state” is started and this state lasts until the value of a becomes less than $0.5S_m$. The value of stress and strain corresponding to the “principal points” in “multiple cracking state” is calculated by the following formulas:

$$esm(2 < i < N-1) = \left(\frac{1+n\rho \cosh(ka)}{n\rho \cosh(ka)-1} \right) \cdot \left(\frac{\sqrt{1+.5\cosh(2ka)-\frac{.75\sinh(2ka)}{ka}}}{(\cosh(ka)-1)n\rho} \right) \cdot (\varepsilon'_{cr} (\exp(-550 \cdot esm(i) - \varepsilon'_{cr}))) \quad (19)$$

$$scm(2 < i < N-1) = \left(\frac{\sqrt{1+.5\cosh(2ka)-\frac{.75\sinh(2ka)}{ka}}}{\cosh(ka)-1} \right) (f'_t (\exp(-550esm(i) - \varepsilon'_{cr}))) \quad (20)$$

Eqs. (19) and (20) are derived from Eqs. (8) and (10), respectively; in which the value of the concrete tensile strength is predicted by an empirical formula; this formula have been suggested by Gupta and Maestrini (1990); in that, “damage index” or C is considered to be equal to 550; this value has been chosen according to Choi and Cheung (1996). Parameter a is the half of the spacing between the two faces of two adjacent cracks in a tensile member; the value of $2a$ for the first “principal point” of “multiple cracking state” ($i=3$) is equal to element length perpendicular to crack direction, L ; for the second point of “multiple cracking state”, $i=4$, the value of parameter $2a$ is bisected and it gets the value of $L/2$; for the next points this procedure will be continued until a becomes less than half of the average final crack spacing (S_m); at this point ($i=N-1$) which is called “final cracking point”, the “multiple cracking” curve is completed. It is clear that Eq. (19) should be solved by an iterative scheme.

At “final cracking state”, the curve corresponding to this part is idealized by a line which is defined by two points, namely, “final cracking point” ($i=N-1$) and “ultimate tensile point” ($i=N$). At this stage, $\{esm\}$ and $\{scm\}$ vectors are computed by these two formulas:

$$esm(i=N-1) = \varepsilon_y - \frac{f_{bu}\Psi \cdot S_m}{A_s E_s \cdot 2\sqrt{3}} \quad (21)$$

$$scm(i=N-1) = 0.577f'_t \exp(-550(esm(i) - \varepsilon'_{cr})) \quad (22)$$

For simplicity and due to the lack of information about corrosion effect on “final cracking state”, the “final cracking state” is neglected for corroded RC elements, therefore, Eqs. (21) and (22) change to:

$$esm(i=N-1) = \varepsilon_y, \quad scm(i=N-1) = 0 \tag{23}$$

and the “final tensile point” is calculated by:

$$esm(i=N) = \varepsilon_y, \quad scm(i=N) = 0 \tag{24}$$

A comparison between Eqs. (23) and (24) shows that the elements $i = N-1$ and N has the same values for the corroded RC elements, leading to removal of the “final cracking state”.

2.4. Verifications

The performance of the proposed model is verified by comparison between analytical and experimental results. Physical and mechanical properties of Wollrab, *et al.* (1996) and Rizkalla and Hwang (1984) specimens presented in Table 1; also, the geometry of the specimens can be found in Fig. 8. Since the proposed model is to be used for rectangular RC shell elements in a finite element modeling, it is expected that the proposed tension-stiffening model works for rectangular RC

Table 1 Physical and mechanical properties of non-corroded experimental specimens, adopted from Wollrab, *et al.* (1996) and Rizkalla and Hwang (1984)

	Wollrab, <i>et al.</i>	Rizkalla and Hwang
d , mm	6.0	11.2776
Number of reinforcement (m)	7	8
E_s , MPa	223480.0	203890.3
f_y , MPa	506.0	461.92
f_c , MPa	44.0	55.78
f'_t , MPa	3.19	2.98
E_c , MPa	30353.0	35694.8639
c , mm	22.4	19.05
E_b , MPa/mm	350.0	138.40
f_{bu} , MPa	4.5	4.57
L , mm	435.0	762.0
A_g , mm ²	107×50.8 (First Crack) 127×50.8 (Other Cracks)	304.8×177.8

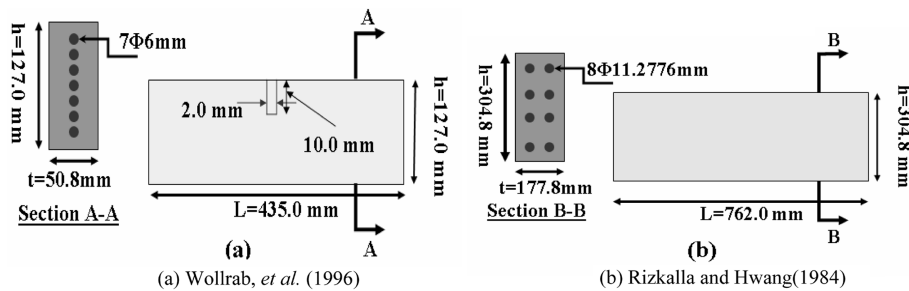
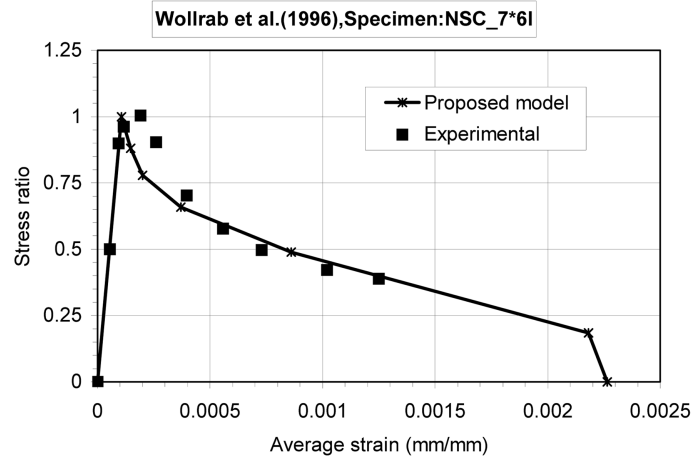
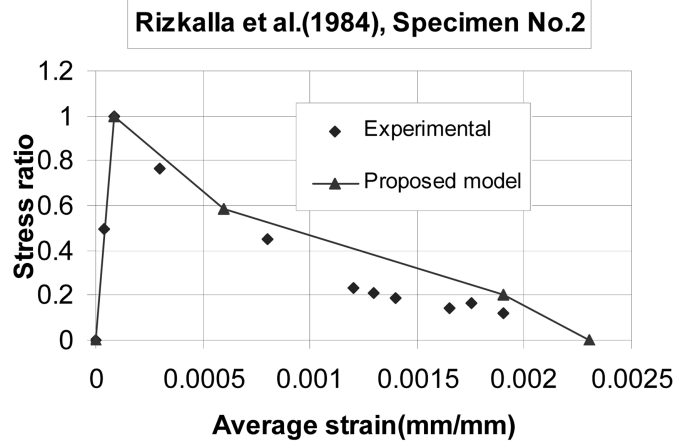


Fig. 8 Experimental specimens of Wollrab, *et al.* (1996) and Rizkalla and Hwang (1984)



(a) Wollrab, *et al.* (1996)



(b) Rizkalla and Hwang (1984)

Fig. 9 Comparison between experimental and analytical results

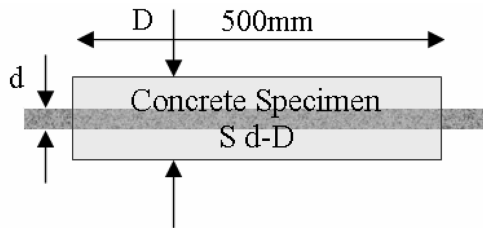


Fig. 10 Experimental specimen of Ghalehnovi (2004)

elements reasonably as shown in Fig. 9.

Three corroded cylinder RC specimens have been chosen (Ghalehnovi 2004). Physical and mechanical properties of specimens are available in Fig. 10 and Table 2. The proposed tension-stiffening model for these three specimens are compared with the results of the experimental observations as reported in Fig. 11.

Table 2 Physical and mechanical properties of corroded experimental specimens

	S18-100-3	S18-100-6	S25-100-6
d , mm	18.0	18.0	25.0
C_w , %	7.0	13.0	11.0
E_s , MPa	200000.0	200000.0	202000.0
f_y , MPa	350.0	350.0	369.0
f_c , MPa	26.0	26.0	26.0
f_t' , MPa	1.62	1.62	1.62
E_o , MPa	24400.0	24400.0	24400.0
c , mm	41.0	41.0	37.5
E_b , MPa/mm	350.0	350.0	350.0
f_{bw} , MPa	4.65	4.65	3.06
L , mm	500.0	500.0	500.0

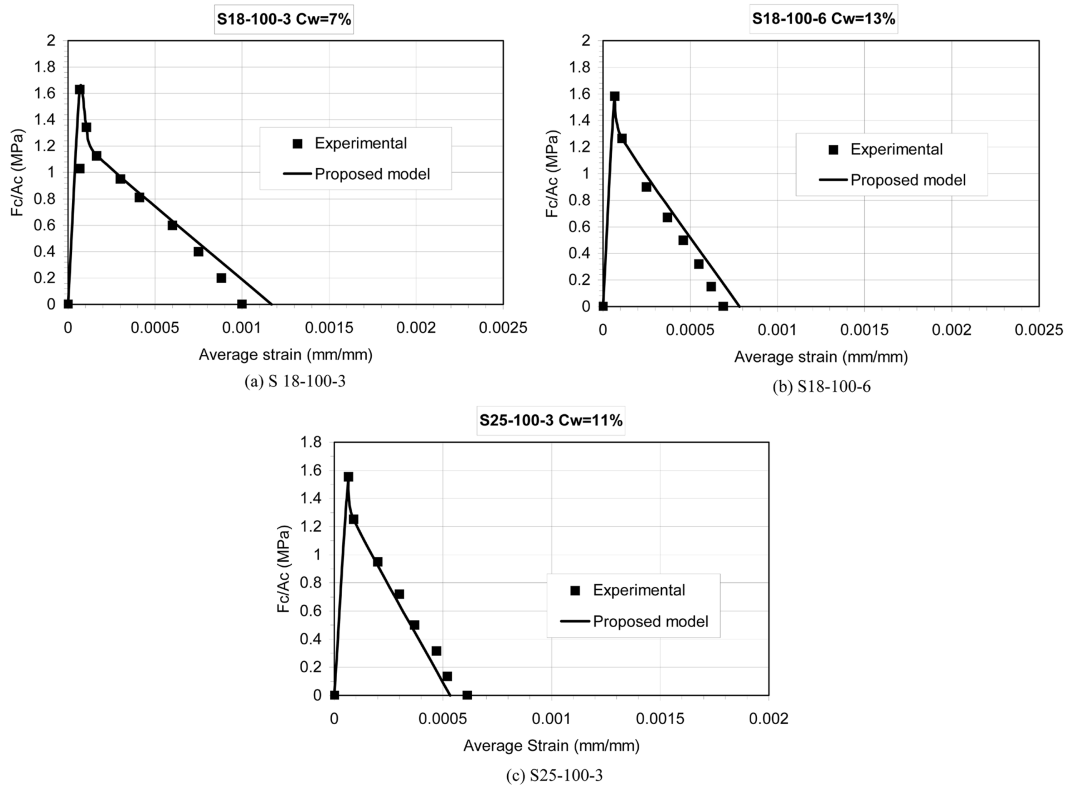


Fig. 11 Comparison between experimental and analytical results

3. Comparison of predictions and experimental results

The proposed tension stiffening model is implemented into a nonlinear finite element analysis program which is called HODA. The abilities of the developed program on the analysis of the field corroded RC beam specimens are performed as follows:

3.1. The finite element program

The history, capabilities, element library, constitutive models and limitations of HODA nonlinear finite element analysis program used in this study are extensive and those are discussed by Shayanfar (1995). This program can depict, through the entire monotonically increasing load range, the static and reversed cyclic response of any plain, reinforced or prestressed concrete structures that is composed of thin plate members. This includes beams, slabs (plates), shells, folded plates, box girder, shear walls, or any combination of these structural elements. Time-dependent effects such as creep and shrinkage can be also studied. The element library includes membrane, plate bending, facet shell, one-dimensional bar, and boundary elements. Fig. 12 shows facet element and associated degree of freedoms which has been used for modeling the RC beams. The program employs a layered finite element approach. The structure is idealized as an assemblage of thin constant thickness plate elements with each element subdivided into a number of imaginary layers as shown in Fig. 12. Each layer is assumed to be in plane stress condition, and can be in any state - uncracked, partially cracked, fully cracked, non-yielded, yielded, and crushed- depending on the stress or strain conditions. Analysis is performed using an incremental-iterative tangent stiffness approach, and the stiffness of the element is obtained by adding the stiffness contributions of all layers at each Gauss quadrature point. Appropriate convergence/divergence criteria are utilized to stop the iterations in each load step as soon as a required degree of accuracy has been attained. Concrete are assumed to be as a stress-induced orthotropic material. The hypoelasticity constitutive relationship developed by Shayanfar (1995) has been used for modeling of the uncracked concrete. Smearred crack approach has been adopted for modeling of the cracked concrete. Thorenfeldt, *et al.* (1987) relationship which is able to accurately represent the family of stress-strain curves for different strength concretes including the high strength concrete is employed. In this research, the program has been modified to include tension-stiffening effect considering bond-slip and corrosion effects in reinforced concrete structures. The steel reinforcement is treated in HODA program as an elasto-plastic-strain-hardening material. A slightly modified form of the biaxial strength envelope curve developed by Kupfer, *et al.* (1969) is used in the program built up in the present study.

3.2. Description of RC beams

Three reinforced rectangular beams with f'_c equal to 70.1 MPa – that are almost high strength

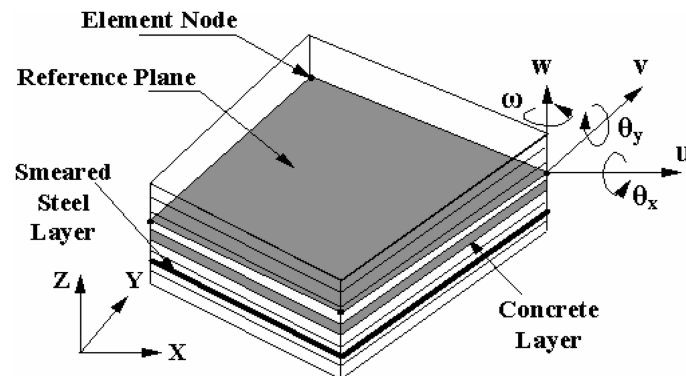


Fig. 12 Facet shell element and associated degree of freedoms

type concrete- were tested by Lee, *et al.* (2000). Three beam specimens of their tests, namely BCD1, BCD2 and BCD3 are investigated in this study. The beams were 250×200 mm² in cross-section and they were supported over a clear span of 2000 mm (see Fig. 13). It was subjected to two concentrated loads. The details of the reinforcement layout and the geometry of the beams are shown in Fig. 13. The material properties of the concrete and the steel reinforcement are given in Table 3. The rate of reinforcement corrosion of each specimen is available on Table 4.

3.3. Finite element modeling

Because of symmetry of load and geometry of the beams, only one-half of the beams are modeled in the finite element idealization. The beam specimen is discretized into 120 facet shell elements as illustrated in Fig. 13. The Quadrilateral shell element, an inplane membrane element, with 3 degrees of freedom per node (u, v, ω), and the rectangular bending element with 3 degrees of freedom per node (θ_x, θ_y, w) are used. These two types of elements are combined to form a facet shell element; see Fig. 12. Plane stress conditions are assumed, therefore only one layer of concrete is sufficient. The longitudinal reinforcements are modeled using discrete bar elements without any flexural stiffness and are lumped in single bars at the reference surfaces. A 4×4 Gauss quadrature is used for estimating the integrations involved. The vertical loads are applied in 30 load steps with smaller increments of loads being applied just before the beam reaches its ultimate load stage. It would improve the rate of convergence of the solution and the accuracy in predicting the failure load. The smeared fixed crack model is used for crack modeling.

All of the elements classified into two groups according to their tensile behavior; first group consists of reinforced elements with “tension-stiffening” behavior according to the proposed model;

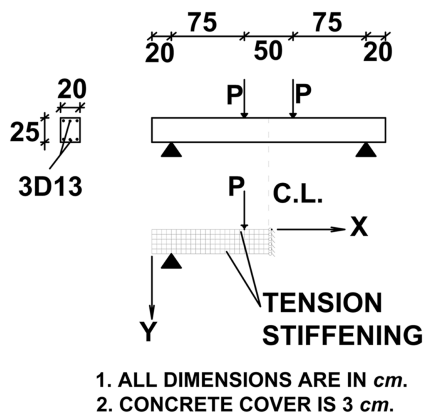


Fig. 13 BCD1, BCD2 and BCD3 experimental details and finite element idealization

Table 3 Material properties of RC beams

Properties	Beams
A_s (mm ²)	256.46
f_c (MPa)	70.1
E_0 (MPa)	38500
ϵ_c	0.002
ϵ_{cu}	0.004 (Assumed value)
f_t' (MPa)	3.67
f_y (MPa)	359.4
E_s (MPa)	197000
E_s^* (MPa)	1300 (Assumed value)
ϵ_{su}	0.15
E_b (MPa/mm)	450 (Assumed value)

Table 4 Rate of corrosion in RC beams

Beams	C_w (%)
BCD1	3.8
BCD2	7.9
BCD3	25.3

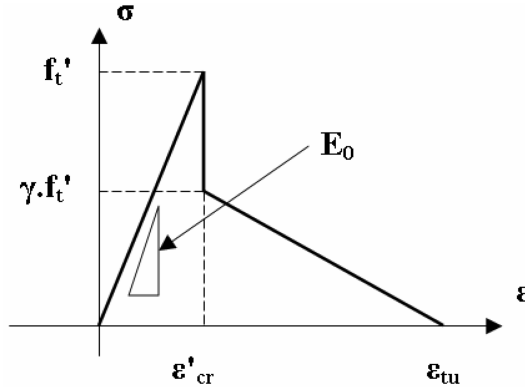


Fig. 14 Tension softening behavior and the associated parameters

second group, consists of elements without reinforcement and their tensile stress-strain curves are described by “tension-softening” behavior similar to Fig. 14. The first group ultimate tensile strain is equal to reinforcement yielding strain, while for the second group, it was chosen near to the strain calculated by a simple formula proposed by Shayanfar, *et al.* (1997); this formula defines the RC element ultimate tensile strain as function of element size in a very simple manner. This is used to remedy mesh size dependency in a nonlinear finite element formulation for reinforced concrete structures. The parameter, γ -see Fig. 14- has been selected equal to 0.25, 0.25 and 0.33, respectively for specimens BCD1, BCD2 and BCD3 to reach a better numerical response. This parameter defines the value of sudden drop after the first tensile crack. This type of modeling -classifying the elements according to their tensile behavior- is similar to what has been proposed by Okamura and Kim (2000), referred to as “zoning method”.

3.4. Computed response of beams BCD1, BCD2 and BCD3

The analytical and experimental load-deflection curves for the beams BCD1 to BCD3 are plotted in Fig. 15. The analytical results are a little bit stiffer than the experimental results and in good agreement with experimental findings. The experimental and analytical results are compared in Table 5. The stiffer response of model can be related to non-uniform corrosion, pitting, and longitudinal cracking due to rebar corrosion and the other items that arise from haphazard nature of corrosion and cracking phenomenon in RC members.

4. The proposed tension-stiffening model shortcomings

The promise of the research was to bring the finite element method to a level in which the performance of a corroded RC member could be evaluated in a reasonable manner. In this regard, the most critical aspect of the modeling is how to take into account the bond strength degradation as result of the corrosion of steel reinforcements. To consider these effects, a new bond-slip-tension-stiffening model was proposed. This owns its unique merits, but the following issues might be set forth for discussions:

- (i) *Experimental study*: The relevant experimental study used in this investigation was limited to

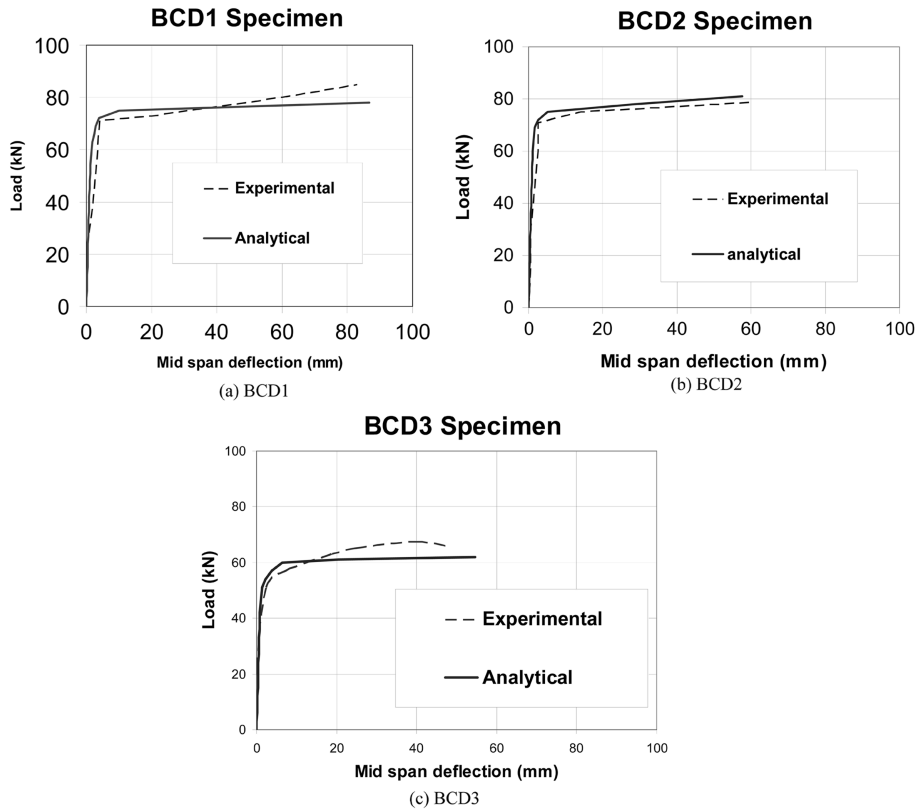


Fig. 15 Experimental and analytical comparison

Table 5 Comparison between experimental and predicted results, all forces are in KN and displacements in mm

Specimen	Experimental				Predicted				Error, %			
	P_y	Δ_y	P_u	Δ_u	P_y	Δ_y	P_u	Δ_u	P_y	Δ_y	P_u	Δ_u
BCD1	71.1	5.0	85.4	83.0	72.0	3.91	78.0	86.6	1.3	21.8	8.7	4.3
BCD2	69.6	4.0	78.8	60.0	72.0	3.42	81.0	57.64	3.0	14.5	2.7	3.9
BCD3	51.5	2.87	65.7	48.2	54.0	2.125	62.0	54.67	4.9	26.0	5.6	13.42

concrete with an ordinary nominal strength.

- (ii) *Transfer length*: Adjacent to the cracked concrete, the slips are much more significant; this length is known as “transfer length”. It had been introduced in development of some of the rational tension stiffening models; e.g. Choi and Cheung (1996). More details about “transfer length” and its effects on RC tensile behavior could be found for example by referring to Somayaji and Shah (1981) or Choi and Cheung (1996). Anyhow, the “transfer length” could be employed in a bond-slip-tension-stiffening model for these two main purposes: (i) to represent the bond stress distribution between reinforcement steel and surrounding concrete, and (ii) to predict the initiation of the final cracking state. In the proposed tension-stiffening model, a linear bond-slip behavior was adopted for multiple cracking state; therefore, the distribution of bond stress

over the reinforcement approaches to the zero value outside the transfer lengths; this per se resembles the condition of the perfect bond there. Furthermore, a simple experimental formula has been employed in the proposed tension stiffening model and a lower limit for the space between two sequential cracks, $2a$, has been defined; this criterion has been utilized to predict the onset of the final cracking state. Based on these arguments, there was no need to pay heed to the subject of “transfer length” in the proposed tension stiffening model.

5. Conclusions and summary

In this paper, a new semi-analytical model describing the tension-stiffening phenomena considering bond-slip behavior and corrosion is represented. The model splits the tension-stiffening curve into two states, namely: “multiple cracking state” and “final cracking state”. The proposed procedure predicts the “final cracking point” by an experimental criterion by setting a lower bound for the average final crack spacing parameter. Another novel aspect of the tension-stiffening model is the discretization of the tension-stiffening curve by a set of points called “principal points” and using linear interpolation technique for computing tensile stress corresponding to a specific tensile strain. This model has been implemented into the HODA program. This program utilizes the hypoelastic model and the smeared crack approach. The hypoelastic models have better performance than the plasticity models from accuracy and eco-numerical points of view for concrete structures. The model has been tested by means of analyzing three field RC beams; the RC beams have the same geometry and material property but different rates of tensile rebar corrosion. The analytical responses using HODA program reveals good agreements with the experimental findings. The principal features of this paper in a quick view are:

- (i) Without using any special element between concrete and steel by only modifying the tension-stiffening curve depending on the rate of steel bar corrosion, the corroded RC elements can be modeled with a reasonable accuracy. This method is applicable for a vast variety of steel reinforcement corrosion rates.
- (ii) A new bond-slip-tension-stiffening algorithm has been introduced.
- (iii) Ductility and the failure points of the corroded reinforcements RC members have been predicted reasonably by the means of a simple nonlinear finite element model.

Notations

a	= half of space between to sequential crack
A_s	= area of reinforcements in a element
A_{s0}	= area of reinforcements in a element without considering corrosion
A_c	= net cross-sectional area of concrete specimen
A_g	= gross area of concrete specimen
c	= rebar cover
C	= damage index
C_1	= a constant value
C_w	= rate of corrosion
d	= diameter of reinforcement
d_0	= the average diameter of reinforcements in one element without considering corrosion

D	= diameter of concrete specimen
$\{esm\}$	= principal tensile strain vector
E_b	= initial moduli of bond-slip curve
E_0	= initial moduli of stress-strain curve of concrete
E_s	= initial tangent modulus for reinforcing steel
E_s^*	= tangent moduli for reinforcing steel in strain hardening region (bi-modulus)
F_c	= concrete force contribution
F_{cm}	= average concrete force contribution
F_s	= steel reinforcement force contribution
F_{sm}	= average steel reinforcement force contribution
f_b	= bond strength
f_{bu}	= ultimate bond strength
f_c	= concrete uniaxial compressive strength
f_u	= rebar ultimate strength
f_t	= concrete tensile strength
f_t'	= concrete uniaxial tensile strength
f_y	= yield strength of reinforcing steel
h	= width
i	= counter
k	= tension stiffening parameter
L	= length
n	= ratio of initial steel moduli of elasticity to concrete one's
N	= length of principal tensile stress or strain vectors
P	= applied load
P_u	= ultimate load
P_y	= yield load
r	= total number of crack in a specimen
S_i	= final crack spacing as per Fig. 5
S_m	= average final crack spacing
$\{scm\}$	= principal tensile stress vector
t	= thickness
T	= tensile force
u, v, w	= displacements in X, Y, and Z directions
U_1, U_2	= strain energy
z	= an axis perpendicular to crack direction
Δ_u	= ultimate displacement
Δ_y	= yielding displacement
ε	= strain
ε_c	= concrete strain corresponding to concrete compressive strength
ε_{cu}	= ultimate compressive strain in concrete
ε_{cr}	= cracking strain of concrete
ε_{cr}'	= concrete uniaxial tensile cracking strain
ε_{su}	= ultimate steel reinforcement strain
ε_{sm}	= average steel reinforcement strain contribution
ε_{tu}	= ultimate concrete tensile strain

ε_y	= yielding strain of steel reinforcement
γ	= softening parameter
$\theta_x, \theta_y, \omega$	= rotations about X, Y and Z axes
ρ	= reinforcement ratio or A_s/A_c
σ	= stress
σ_{ic}	= concrete stress contribution in tension
σ_{icm}	= mean concrete stress contribution in tension
$\sigma_{ic, \max}$	= maximum concrete stress contribution in tension between two faces of subsequent cracks
Ψ	= rebar average perimeter

References

- Amleh, L. and Mirza, M. S. (1999), "Corrosion influence on bond between steel and concrete", *ACI Struct. J.*, **96**(3), 415-423.
- Choi, C. K. and Cheung, S. H. (1996), "Tension stiffening model for planar reinforced concrete members", *Comput. Struct.*, **59**, 179-190.
- Coronelli, D. and Gambarova, P. (2004), "Structural assessment of corroded reinforced concrete beams: Modeling Guidelines", *J. Struct. Eng., ASCE*, **130**(8), 1214-1224.
- Dekoster, M., Buyle-Bodin, F., Maurel, O. and Delmas, Y. (2003), "Modeling of the flexural behavior of RC beams subjected to localized and uniform corrosion", *Eng. Struct.*, **25**, 1333-1341.
- Ghalehnovi, M. (2004), "Characteristic relations in nonlinear finite element analysis with considering corrosion and bond-slip", *PhD thesis*, Iran University of Science and Technology, Tehran, Iran (In Persian).
- Gupta, A. K. and Maestrini, S. R. (1990), "Tension stiffness model for cracked reinforced concrete", *J. Struct. Eng. ASCE*, **116**(3), 769-790.
- Kupfer, H. B., Hildsford, H. K. and Ruch, H. (1969), "Behavior of concrete under biaxial stresses" *ACI J.*, **66**(8), 656-66.
- Lee, H. S., Noguchi T. and Tomosawa F. (2000), "Analytical evaluation of structural performance of reinforced concrete beams considering degree of reinforcing bar corrosion", *Proceedings of Fourth International Conference on Repair, Rehabilitation and Maintenance of Concrete Structures and Innovations in design and Construction, Seoul, Korea*, **SP 193-46**, 779-789.
- Lundgren, K. (1999), "Three dimensional modeling of bond in reinforcement concrete, theoretical model, experiment and applications", PhD thesis, Department of Structural Engineering, Chalmers University of Technology, Gotenberg, Sweden.
- Lundgren, K. (2001), "Bond between corroded reinforcement and concrete", Report No.00:3, Department of Structural Engineering, Chalmers University of Technology, Gotenberg, Sweden.
- Okamura, H. and Kim, I. H. (2000), "Seismic performance check and size effect FEM analysis of reinforced concrete", *Eng. Fracture Mech.*, **65**, 369-389.
- Rizkalla, S. H. and Hwang, L. S. (1984), "Crack prediction for members in uniaxial tension", *ACI J.*, **81**, 572-579.
- Shayanfar, M. A. (1995), "Nonlinear finite element analysis of normal and high strength concrete structures", PhD thesis, McGill University, Montreal, Canada.
- Shayanfar, M. A., Kheyroddin, A. and Mirza, M. S. (1997), "Element size effects in nonlinear analysis of reinforced concrete members", *Comput. Struct.*, **62**(2), 339-352.
- Somayaji, S. and Shah, S. P. (1981), "Bond stress versus slip relationships and cracking response of tension members", *ACI J.*, **78**, 217-225.
- Thorenfeldt, E., Tamaszemicz, A. and Jenson, J. J. (1987), "Mechanical properties of high strength concrete and application in design", *Proceedings of International Symposium on Utilization of High Strength Concrete, Stavanger, Norway*, 149-159.
- Wollrab, E., Kulkarni, S. M., Ouyang, C. and Shah, S. P. (1996), "Response of reinforced concrete panels under uniaxial tension", *ACI Struct. J.*, **93**(6), 648-657.